Eur J Nucl Med Mol Imaging (2014) 41 (Suppl 1):S115–S124
DOI 10.1007/s00259-013-2675-5

REVIEW ARTICLE

The role of SPECT/CT in radioembolization of liver tumours

Hojjat Ahmadzadehfar · Heying Duan · Alexander R. Haug · Stephan Walrand · Martha Hoffmann

Received: 13 December 2013 / Accepted: 17 December 2013 / Published online: 18 January 2014

Abstract Radioembolization (RE) with ^{90}Y microspheres is a promising catheter-based therapeutic option for patients with unresectable primary and metastatic liver tumours. Its rationale arises from the dual blood supply of liver tissue through the hepatic artery and the portal vein. Metastatic hepatic tumours measuring >3 mm derive 80 – 100 % of their blood supply from the arterial rather than the portal hepatic circulation. Typically, an angiographic evaluation combined with ^{99m}Tc-macroaggregated albumin (^{99m}Tc-MAA) scan precedes therapy to map the tumour feeding vessels as well as to avoid the inadvertent deposition of microspheres in organs other than the liver. Prior to administration of ^{99m}Tc-MAA, prophylactic coil embolization of the gastroduodenal artery is recommended to avoid extrahepatic deposition of the microspheres. SPECT/CT allows direct correlation of anatomic and functional information in patients with unresectable liver disease. SPECT/CT is recommended to assess intrahepatic distribution as well as extrahepatic gastrointestinal uptake in these patients. Pretherapeutic SPECT/CT is an important component of treatment planning including catheter positioning and dose finding. A post-therapy bremsstrahlung (BS) scan should follow RE to verify the distribution of the administered tracer. BS SPECT/CT imaging enables better localization and definition of intrahepatic and possible extrahepatic sphere distribution and to a certain degree allows posttreatment dosimetry. In this paper we address the usefulness and significance of SPECT/CT in therapy planning and therapy monitoring of RE.

Keywords SPECT/CT · Radioembolization · Liver tumours · 90Y microspheres

Hojjat Ahmadzadehfar and Heying Duan contributed equally to this work.

H. Ahmadzadehfar
Department of Nuclear Medicine, University Hospital Bonn, Bonn, Germany

H. Duan · A. R. Haug · M. Hoffmann (✉)
Department of Biomedical Imaging und Image-guided Therapy, Clinical Division of Nuclear Medicine, Medical University of Vienna, Waehringer Guertel 18-20, 1090 Vienna, Austria
e-mail: martha.hoffmann@meduniwien.ac.at

S. Walrand
Nuclear Medicine, Université Catholique de Louvain, Brussels, Belgium

Introduction

Radioembolization (RE), also called selective internal radiation therapy (SIRT) or transarterial RE (TARE), is a promising catheter-based liver-directed therapy for patients with primary and metastatic liver cancer [1–3]. RE provides several advantages over traditional treatment methods, including a low toxicity profile [4, 5]. Its rationale arises from the anatomic and physiological nature of hepatic tumours. The prominent feature is the dual blood supply of liver tissue, from the hepatic artery and the portal vein. Approximately 70 % and 30 % of hepatic blood is derived from the gastrointestinal (GI) tract via the portal vein and the systemic circulation via the hepatic artery, respectively [6]. Metastatic hepatic tumours measuring >3 mm derive 80 – 100 % of their blood supply from the arterial rather than the portal hepatic circulation [6].

In addition to RE with ^{90}Y microspheres, various other radionuclides have also been considered for treatment of liver tumours including ^{32}P, ^{188}Re and ^{166}Ho [7–10]. In this paper, however, we focus on glass and resin ^{90}Y microspheres, which are FDA-approved medical devices. ^{90}Y is a pure β-emitter, produced by neutron bombardment of ^{89}Y in a reactor, with a limited tissue penetration (mean 2.5 mm, maximum 11 mm) and a short half-life of 64.2 h, thus making it an ideal transarterial liver-directed agent [11]. Two ^{90}Y microsphere

products are commercially available today: TheraSphere® (glass microspheres) and Sir-Spheres® (resin microspheres). There are some distinct differences between the two products discussed in detail elsewhere [11].

In the process of selecting patients referred for RE, several aspects should be considered: Patients eligible for RE should present with an unresectable hepatic primary or metastatic cancer, liver-dominant disease, a life expectancy of at least 3 months and an ECOG performance score of ≤2 as well as preserved liver function [12]. Overall, the incidence of complications of RE of liver malignancies for appropriately selected patients and accurately targeted delivery is very low [13]. Serious complications have been reported when microspheres were inadvertently deposited in excessive amounts in organs other than the liver or when exceeding the radiation tolerance levels of the liver, leading to RE-induced liver disease (REILD) [14]. Radiation and diminished blood supply due to embolization and subsequent hypoxia or possible reflux of ^{90}Y microspheres into the gastroduodenal circulation may result in ulceration and even perforation of the stomach and duodenum [14, 15], that may subsequently require surgery [16]. Reported complications include GI ulceration/bleeding, gastritis/duodenitis, cholecystitis, pancreatitis, radiation pneumonitis and hepatic decompensation [5, 12, 14–20]. The decision to perform RE should be based on an interdisciplinary consensus in an adequate tumour board with participation of specialists in surgery, gastroenterology, oncology, radiology, nuclear medicine and radiation therapy.

An angiographic evaluation combined with ^{99m}Tc-macroaggregated albumin (^{99m}Tc-MAA) imaging precedes the therapy session (test angiogram) to map the tumour-feeding vessels as well as to avoid the complications mentioned above. It is well known that the anatomy of the mesenteric system and the hepatic arterial bed has a high degree of variation, with the "typical" vascular anatomy being present in only 60 % of cases [21]. Therefore, ^{99m}Tc-MAA scintigraphy has been primarily used to identify and calculate excessive liver-to-lung shunt volume. The additional use of SPECT/CT allows a direct correlation of anatomic and functional information. This ^{99m}Tc-MAA SPECT/CT scan allows not only assessment of the intrahepatic microsphere distribution but also detection of extrahepatic uptake [22–26].

It is also recommended that RE is followed by a posttherapy bremsstrahlung (BS) scan to verify the distribution of the administered tracer [27]. Even though the quality of BS images is low due to the characteristics of BS, BS SPECT/CT enables better localization and definition of the intrahepatic and possible extrahepatic distribution of spheres [28–31]. In this paper, we address the usefulness and significance of SPECT/CT imaging in therapy planning and therapy monitoring of RE.

^{99m}Tc-MAA SPECT/CT for treatment planning

In the test angiogram session 150 – 200 MBq of ^{99m}Tc-MAA is injected selectively into the right and/or left hepatic artery or even into segmental arteries. If required by the specific vascular anatomy, prophylactic coil embolization of the gastroduodenal artery and optionally the right gastric artery and its pancreaticoduodenal branches is recommended prior to ^{99m}Tc-MAA administration to avoid extrahepatic deposition of microspheres according to the vessel anatomy [12]. Of note, these vessels/organs can revascularize rapidly, and therefore the embolization should be performed close to the intended time of RE. It is necessary to angiographically re-evaluate vascularity and blood supply during RE to ensure that such revascularization has not occurred [12]. Prior to the test angiogram session oral administration of 600 mg perchlorate at least 30 min before ^{99m}Tc-MAA administration is recommended by the German radiation protection commission [32] in order to avoid nonspecific tracer uptake in the stomach due to free ^{99m}Tc-pertechnetate [33]. The ^{99m}Tc-MAA should be administered slowly without pressure and the syringe should be gently tilted before injection to agitate sedimented ^{99m}Tc-MAA particles [34].

First, a whole-body scintigraphy scan in the anterior and posterior projection should be obtained to calculate the percentage of potential tracer uptake in the lungs (liver-to-lung shunt volume). Second, SPECT/CT images should be obtained. To date there are no definitive recommendations for ^{99m}Tc-MAA SPECT/CT acquisition and reconstruction parameters, and consequently different protocols are in use. Irrespective of the variety of acquisition protocols a low-energy high-resolution (LEHR) collimator should be used with the energy window set at 140 keV ±10 %. SPECT acquisition should be performed with a 128×128 or 256×256 matrix with 3° steps (15 – 30 s per projection). In some centres the acquisition is performed with fewer steps (6° steps) or a shorter acquisition time or even a smaller matrix size [35]. A diagnostic contrast-enhanced CT scan including an arterial phase is required for evaluating the intrahepatic tumour distribution as well as for measuring tumour volume, and also to ascertain the vascular situation. If the contrast-enhanced CT scan precedes the inclusion to RE, then the CT part of the SPECT/CT could be performed with lower-quality settings, such as with 5-mm slices. In that case it is recommended that the SPECT images be fused with these previously obtained contrast-enhanced CT images or magnetic resonance images (MRI).

Evaluation of extrahepatic tracer deposition

Using only planar images for detecting hot-spots in other organs besides the liver is of limited value due to the limited spatial resolution. Extrahepatic spots indirectly mark the

possible locations of microspheres misplaced during therapy; however, planar image analysis can be difficult and lead to misinterpretation of possible extrahepatic locations. Furthermore, especially in the upper abdomen, the localization of several different organs within a relatively small region demands the analysis of tomographic images to differentiate the ^{99m}Tc-MAA accumulation in the liver from that in an adjacent organ [22]. In this regard, ^{99m}Tc-MAA SPECT/CT imaging has been shown to provide more valuable information than planar and SPECT images, and is therefore the imaging modality of choice (Fig. 1a, b) [22–25, 36]. In comparison to planar and SPECT imaging, the use of SPECT/CT can increase the sensitivity of a ^{99m}Tc-MAA scan in the diagnosis of abdominal extrahepatic shunting up to 100 %, thus leading to a change in approach and therapy [22, 24].

RE may cause GI ulcers in up to 4.8 % patients [37]. Radiation-induced ulcers are difficult to treat [37]. The two major causes thought to be responsible for gastroduodenal ulcers are digestive shunting via an aberrant gastroduodenal vessel that receives the microsphere injection, and microsphere reflux during injection [23]. In addition, focally increased GI uptake has been reported in up to 31 % of patients [22–26]. Free ^{99m}Tc uptake of the gastric mucosa may be seen as low to moderately diffuse gastric uptake in SPECT/CT images. Therefore, visual distinction between gastric concentration of free ^{99m}Tc and true gastric ^{99m}Tc-MAA shunting may be challenging, and this considerably reduce diagnostic quality/clinical confidence [33]. In this situation, perchlorate administration prior to the test angiogram is helpful in avoiding any misinterpretation of gastric uptake.

Radiation cholecystitis is usually subclinical, but it is associated with postprocedural morbidity and requires surgical intervention in about 1 % of patients [38]. ^{99m}Tc-MAA accumulation in the gallbladder is seen in 8 – 12 % of patients [22–24]. In these patients subsequent RE is considered controversial with regard to the need for changes in the therapy plan involving prophylactic antibiotic therapy or choelcystectomy (Fig. 1c, d) [22–24]. One strategy to prevent the spheres from reaching the gallbladder resulting in radiation-induced cholecystitis may be the placement of the catheter distal

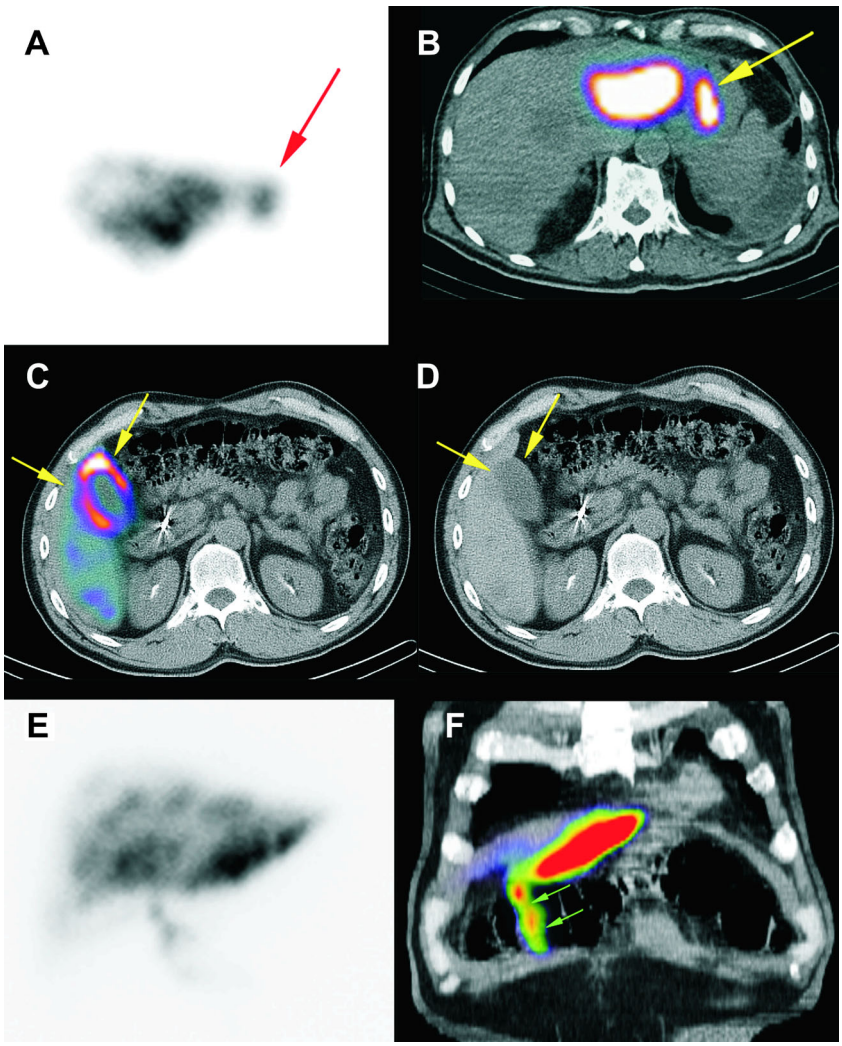

Fig. 1 Extrahepatic tracer accumulation. **a**, **b** ^{99m}Tc-MAA scan in a patient with HCC scheduled for RE of the left liver lobe showing tracer accumulation in the stomach (**b** *yellow arrow*), not distinguishable from intrahepatic accumulation on the planar scan without SPECT/CT imaging (**a** *red arrow*). **c**, **d** Tracer accumulation in the gallbladder wall (*yellow arrows*) in a patient with colorectal carcinoma. **e**, **f** Planar image (**e**) shows ^{99m}Tc-MAA deposition in the anterior abdominal wall, indicating a patent hepatic falciform artery; coronal ^{99m}Tc-MAA SPECT/CT image in the same patient (**f**) localizes the tracer accumulation along the hepatic falciform ligament (*arrows*)

to the cystic artery. We recommend this approach providing it does not lead to inadequate target distribution of microspheres. An alternative approach is the prophylactic embolization of the proximal cystic artery with either absorbable gelatine sponge pledgets or fibred microcoils immediately before RE, which has been shown to be safe and feasible [39].

^{99m}Tc-MAA uptake in the anterior abdominal wall has been described as a sign of a patent hepatic falciform artery (HFA) [40] with a reported incidence of up to 13 % [23, 41–44]. The HFA arises as a terminal branch of the middle or left hepatic artery and runs within the hepatic falciform ligament with the umbilical vein, provides partial blood supply around the umbilicus, and communicates with branches of the internal thoracic and superior epigastric arteries [45]. It is known that influx of chemoembolic agents into the HFA can cause a supraumbilical skin rash, epigastric pain and skin necrosis. Normally, a patent HFA appears on planar ^{99m}Tc-MAA scans as elongated tracer accumulation in the mid-abdomen, which is more correctly localized by SPECT/CT (Fig. 1e, f) [23, 42]. Usually, ^{99m}Tc-MAA uptake via the HFA is easily recognized and does not lead to diagnostic problems except in patients with umbilical hernia [23]. As for all other extrahepatic arteries, prophylactic embolization of the HFA is recommended, yet it is not always possible to delineate and catheterize this small vessel.

Several papers report that RE-related side effects in patients with tracer accumulation in the anterior abdominal wall on the ^{99m}Tc-MAA scan are neither common nor severe [23, 42, 44]. Leong et al. reported one patients with self-limiting radiation dermatitis caused by shunting of ^{90}Y microspheres to the anterior abdominal wall via a patent HFA [46]. In a recent study, a patient HFA was identified by ^{99m}Tc-MAA SPECT/CT in 16 patients who did not undergo coil embolization prior to treatment with only one patient complaining of abdominal pain for 48 h without skin lesions [42]. Therefore, there seems to be no absolute need for prophylactic embolization of either the HFA or modification of the treatment plan if the HFA is not detectable in an angiography session and the intensity of HFA deposition is low. Recently, Lenoir et al. reported tracer uptake in the hepatic artery in 6.6 % of patients [23], which had no impact on patient management. This arterial uptake is likely due to the aggregation of MAA by arterial microlesions caused by long and complicated angiography procedures or when arteries are weakened by previous procedures [23].

Evaluation of intrahepatic tracer distribution

The aim of RE is to treat the total hepatic tumour load while avoiding delivery of particles to healthy liver tissue. In patients with a single liver tumour, intrahepatic accumulation of ^{99m}Tc-MAA could be acceptably assessed by planar images and SPECT. SPECT/CT may be of higher value in patients with multiple liver lesions and lesions adjacent to surrounding structures. For example, ^{99m}Tc-MAA uptake in the tumour thrombus of the portal vein, which is more commonly seen in hepatocellular carcinoma (HCC) [34], can only be detected by SPECT/CT. ^{99m}Tc-MAA uptake in the tumour thrombus is usually a predictor of a favourable response to RE. In a study by Garin et al. [47], 92 % of responding patients with portal vein thrombosis showed ^{99m}Tc-MAA uptake in the thrombosis on SPECT/CT images [47]. There is early proof of a positive correlation between the amount of tumoral ^{99m}Tc-MAA uptake and treatment response, but further clinical studies are needed.

Flamen et al. treated ten patients with colorectal cancer metastases and found that a ^{99m}Tc-MAA tumour to non-tumour (liver) uptake ratio cut-off value of 1 could predict a significant metabolic response [48]. Garin et al. in a study of 36 patients with HCC found that quantitative ^{99m}Tc-MAA SPECT/CT is predictive regarding response, progression-free survival and overall survival. The authors suggested that using tumour dosimetry based on ^{99m}Tc-MAA SPECT/CT imaging could allow adaptation of the treatment plan [47, 49]. The same group reported recently that ^{99m}Tc-MAA SPECT/CT predicted response with a sensitivity of 100 % and overall accuracy of 90 % in 71 HCC patients [50].

A diffuse high accumulation of ^{99m}Tc-MAA in the noninvolved tissue is an important issue, as a high radiation dose to the healthy liver may increase the probability of REILD, a life-threatening condition. The pretreatment angiogram together with the ^{99m}Tc-MAA SPECT/CT provide the opportunity to clearly identify the respective tumour-feeding vessels. This is crucial to avoid excessive radiation exposure to nontarget healthy liver tissue (Fig. 2).

If there is a discrepancy between the segmental distribution of ^{99m}Tc-MAA and the intended vascular territory to be treated, the angiograms should be reviewed carefully. One reason may be tracer injection distal to a branching point, which would exclude part of the tumour area [34], or accessory arterial blood supplying vessels or parasitized arteries [34]. In such cases, the test angiogram should be repeated with more selective ^{99m}Tc-MAA administration into the tumour-feeding arteries followed by SPECT/CT imaging for confirmation of exact targeting.

Pretherapeutic dose estimation and dosimetry

For ^{90}Y-loaded glass microspheres, the dose calculation was based on the accepted simplified formula that includes percentage of pulmonary shunting and the mass of the liver volume to be treated [51]:

$$\mathrm{ILD} = \mathrm{IA} \times (1-\mathrm{S}) \times 50/\mathrm{W}$$

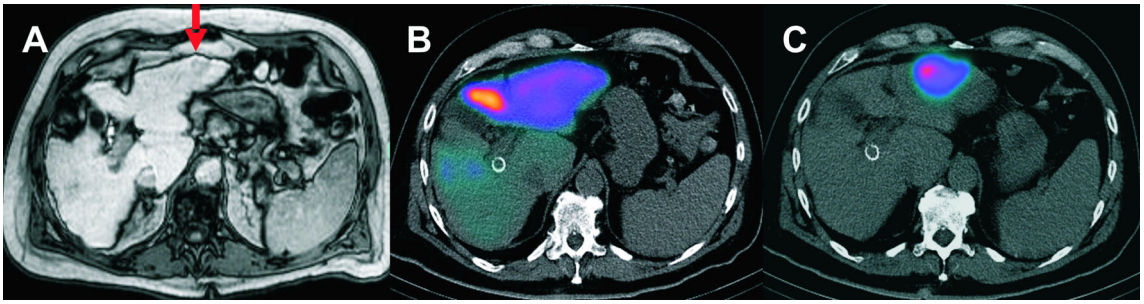

Fig. 2 Patient with HCC in whom RE of a single HCC in the left liver lobe (**a** MRI scan, *red arrow*) was planned. The first test angiogram (**b**) shows diffuse tracer accumulation in the left liver lobe and no specific uptake in the tumour area. The second test angiogram after placing the catheter tip more distally (**c**) shows accentuated accumulation in the tumour area without any relevant uptake in the noninvolved liver

where ILD is the injected liver dose, IA is the injected activity in gigabecquerels, *S* is the percentage of pulmonary shunting as measured by MAA scan, and *W* is the mass in kilograms of the liver volume to be treated. The goal was to deliver a radiation dose of 120±20 Gy to the involved liver volume. For ^{90}Y resin microspheres, two approaches to estimating the needed activity were used: the body surface area (BSA) method and the partition model based on the Medical Internal Radiation Dosimetry (MIRD) methodology. The BSA method uses only the BSA index and the tumour burden to calculate the ^{90}Y activity and thus cannot be considered as a real dosimetry approach. Indeed, it does not take the tumour-to-normal liver activity ratio into account, which is a patient-specific and sometimes a lesion-specific measure of the relative difference in microsphere trapping between tumoral and nontumoral tissue related to their vascularization [52–54]. However, the BSA method is widely used in treatment with ^{90}Y-loaded resin spheres for its simplicity and safety.

The partition method considers the lung, the tumour and the healthy liver as separate compartments, and requires the assessment of the tumour-to-normal liver activity ratio, as well as the tumour and healthy liver mass. As a result, in addition to natural patient variability, anatomic and metabolic effects of previous treatments, such as liver resection and radiofrequency ablation, are taken into account, leading to a more accurate dose estimation [55]. However, this method is limited to well-delineated tumours such as HCC and is of limited value in multiple/disseminated lesions.

Of note, tumour dosimetry should be based on reporting the dose in units of gray rather than megabecquerels per millilitre. For example, a recent study by Van de Wiele et al. in 13 patients showed no significant difference in ^{99m}Tc-MAA specific uptake (median 2 MBq/ml) in responding and nonresponding lesions in RE with glass microspheres [35]. This uptake corresponded to a tumour dose range of 90± 90 Gy. In line with this, Chiesa et al. [56, 57] found in a retrospective study of 52 patients treated with ^{90}Y-loaded glass microspheres an overlap in the absorbed dose of the nonresponding tumours (0 – 500 Gy) and of the responding tumours (250 – 1,500 Gy). In that study, the Liver Normal Tissue Complication Probability (NTCP) strongly depended on the Child Pugh status, with $NTCP_{50}$ occurring around an absorbed dose *D* of 100 Gy for Child Pugh A. This stresses the importance of reporting dosimetry results in gray rather than megabecquerels per millilitre. Another drawback of distribution prediction and dosimetry on the basis of ^{99m}Tc-MAA SPECT/CT is the discrepancy in intrahepatic tracer distribution between before and after treatment.

Chiesa et al. [56] reported the problem of differences in the distribution of ^{99m}Tc-MAA and ^{90}Y microspheres. In 29 patients treated with the same intended catheter positioning as in the pretherapeutic study, the biodistribution was markedly different between the two modalities in two of the 29 patients (7 %). Jiang et al. [58] found a segmental perfusion difference (SPD) between the pre- and posttherapeutic SPECT studies in 31 treatments out of 81, all performed with the catheter in the same intended position. Carefully reanalysing the position of the catheter tip in the two angiograms, they noted only a slight difference in catheter position in 24 of the 31 treatments with SPD, 21 of which showed the catheter tip close to an arterial node. SPD occurred in two treatments despite an identical tip position, also close to an arterial bifurcation. However, for five treatments with SPD no particular explanation could be found. Recently, Wondergem et al. [59] confirmed these features in a similar study.

If at all possible, the catheter tip should be in the same position in the two procedures. However, Jiang et al. also showed that in 9 % of patients (5/57) the SPD could not be explained. A possible explanation can be found in the computer simulations performed by Basciano et al. [60], who found that even for a remote node, the microsphere spreading between daughter vessels depends on the injection time-frame (i.e. during blood acceleration, peak or deceleration), on the injection speed and also on the cross-sectional position of the catheter tip in the artery. The higher number of resin or glass microspheres compared to that of MAA particles could also play a role by differently altering the blood flow during the injection [59]. All these discrepancies are in line with early tumour response studies that displayed a better correlation with the absorbed dose using posttherapy dosimetry [61] than

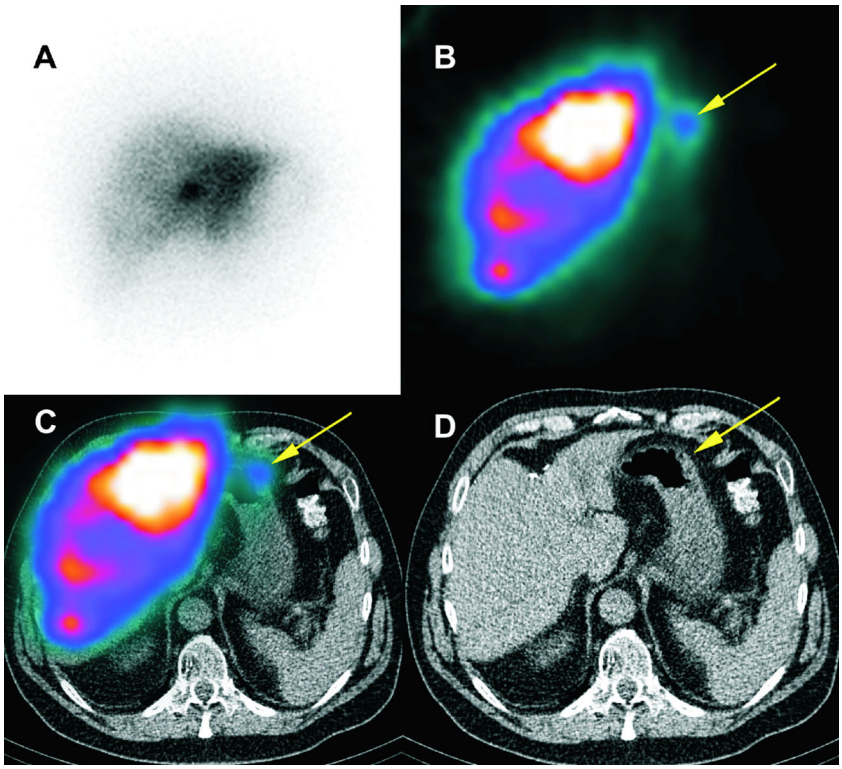

Fig. 3 Whole liver treatment with resin spheres in a 75-year-old patient with cholangiocellular carcinoma (**a** planar BS, **b** BS SPECT, **c** BS SPECT/CT, **d** CT). Due to early onset of flow deceleration until stasis, the administration was terminated (total activity 0.6 GBq). Backflow was not apparent on the angiogram. The planar BS scan shows no pathological findings. The BS SPECT/CT image shows focal gastric accumulation (*arrow*). One week after RE the patient developed gastric pain due to a radiation-induced prepyloric ulcer in the antrum confirmed by gastroduodenoscopy

using pretherapy dosimetry [48]. One might also perform "dosimetry on the fly" by tracking the microsphere deposition during catheterization; this would be a major evolution [62, 63].

Bremsstrahlung SPECT/CT after radioembolization

BS means the photons emitted by beta particles as they lose their energy in tissue [64]. BS imaging should be performed within 24 h of RE. BS SPECT/CT is used to confirm satisfactory microsphere delivery to the target arterial territory. However, no study with a significant number of patients has yet confirmed this. Quantitative evaluation of BS scans with SPECT/CT indicates that this approach may be feasible despite scatter artefacts [31, 65, 66]. Areas of tumour uptake after RE were demonstrated by ^{90}Y BS SPECT/CT in a case reported by Mansberg et al. [30]. According to our experience with BS SPECT/CT, evaluation of tracer deposition in the liver, and especially in metastases, is feasible. Additionally, the absence of ^{90}Y accumulation in a considerable lesion/area correlates well with an unfavourable response.

Although whole-body and planar BS scans can detect diffuse extrahepatic ^{90}Y microsphere accumulation in the lung, intestinal tract, or along the HFA, their analysis may be difficult and misleading due to low spatial resolution. Furthermore, the localization of several different organs within this relatively small region, especially in the upper abdomen, requires analysis of tomographic images to accurately determine whether the ^{90}Y has accumulated in the liver or in an adjacent organ (Fig. 3). Ahmadzadehfar et al. [28] evaluated the significance of BS SPECT/CT in predicting GI ulcers in 188 RE procedures, and observed a dramatic improvement in the accuracy of SPECT/CT compared to SPECT alone. Thus, BS SPECT/CT should be performed after RE to confirm the safe distribution of ^{90}Y microspheres and for the prediction of GI side effects, for an appropriate and timely management strategy if extrahepatic tracer deposition occurs.

Similar to ^{99m}Tc-MAA SPECT/CT, there are no defined instructions for BS acquisitions. The first issue concerning BS imaging is choosing the optimal energy window. Due to the continuous and broad energy distribution of BS photons, and the lack of a well-defined photopeak for ^{90}Y BS imaging, there is significant variability in the acquisition energy window choices [67]. In a phantom study, Ito et al. [68] used three energy window widths of 50 % (57 – 94 keV) centred at 75 keV, 30 % (102 – 138 keV) centred at 120 keV and 50 % (139 – 232 keV) centred at 185 keV set on the ^{90}Y BS spectrum. They found that BS SPECT acquisition using the 120 keV window resulted in the highest spatial resolution and

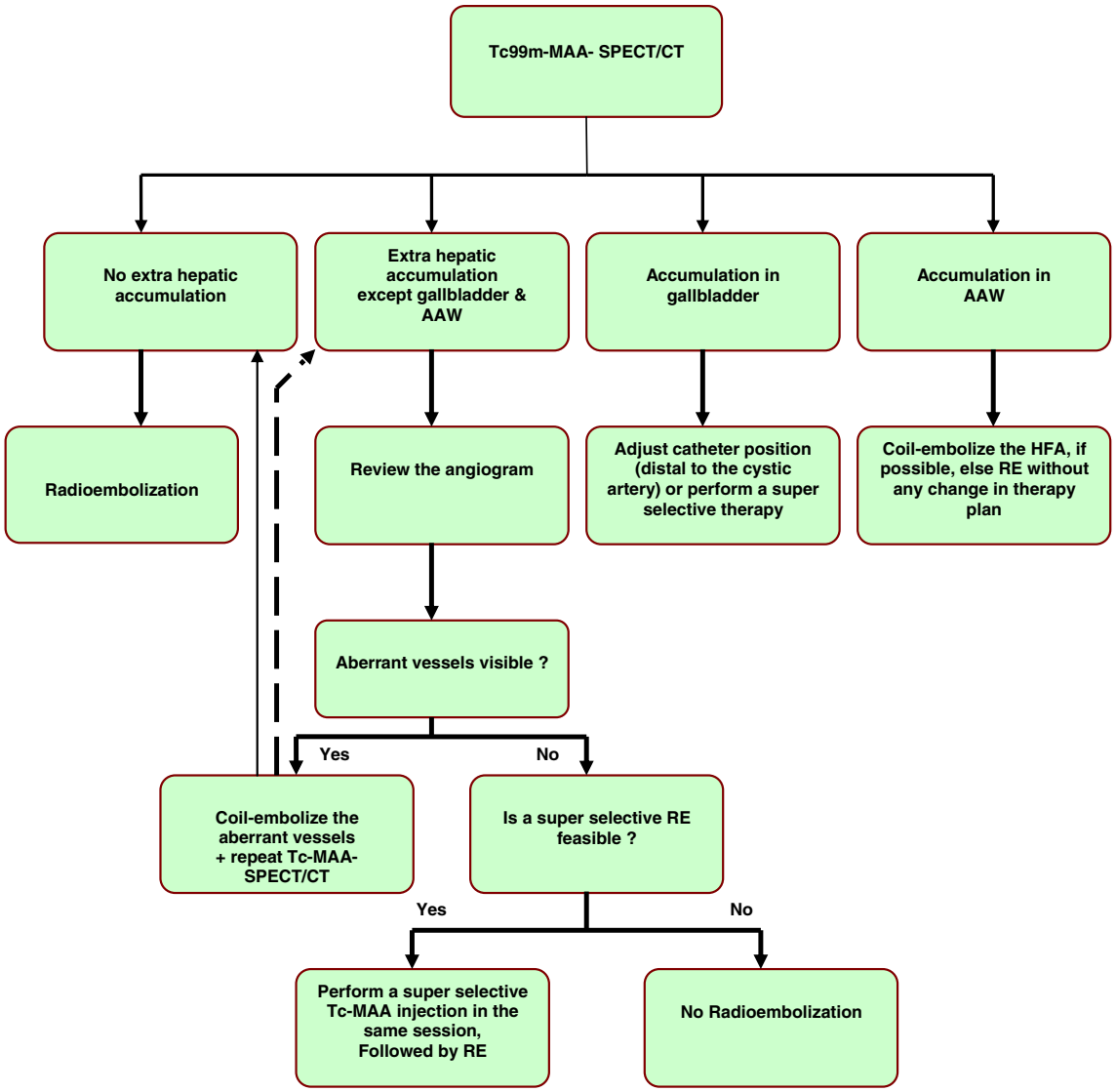

AAW: anterior abdominal wall
RE: radioembolization
HFA: hepatic falciform artery

Fig. 4 Flow chart highlighting the role of SPECT/CT in the treatment pathway. *AAW* anterior abdominal wall, *RE* radioembolization, *HFA* hepatic falciform artery

the lowest diagnostic uncertainty, while the sum window (75, 120 and 185 keV) showed the highest sensitivity (about three times higher than that of the 120 keV window). Most centres use medium-energy, general-purpose collimators (MEGP) [29, 31, 69, 70]. However, there are reports that a high-energy general purpose collimator (HEGP) would also be acceptable [69, 71–73]. For SPECT acquisition, a 128×128 matrix with 64 frames (20 – 30 s per frame) can be used. An iterative reconstruction with attenuation correction may be performed [72, 74]. We recommend using the MEGP, the window centred at 120 keV and iterative reconstruction.

Posttherapeutic dosimetry

Quantitative BS SPECT/CT would require sophisticated correction of intrapatient and intradetector x-ray scattering which are not (yet) commercially available [65, 75, 76]. In contrast,

all PET/CT systems provide the possibility of quantification, so PET/CT will be used more and more in post-RE dosimetry assessment [77–80].

Summary

Pretherapeutic ^{99m}Tc-MAA SPECT/CT and posttherapeutic BS SPECT/CT have been shown to be superior to planar and SPECT imaging alone in treatment planning as well as for post-RE imaging. By using SPECT/CT the efficacy and safety of RE can be improved significantly (Fig. 4). In addition SPECT/CT can improve the pretherapeutic dose estimation with a partition model because of exact delineation of tumoral and nontumoral liver tissue as well as quantification of liver perfusion. Although posttherapeutic dosimetry with BS SPECT/CT might be possible, ^{90}Y PET/CT will probably become the method of choice in post-RE assessment in the near future.

Conflicts of Interest None.

References

1. Sangro B, Carpanese L, Cianni R, Golfieri R, Gasparini D, Ezziddin S, et al. Survival after yttrium-90 resin microsphere radioembolization of hepatocellular carcinoma across Barcelona clinic liver cancer stages: a European evaluation. Hepatology. 2011;54:868–78. doi:10.1002/hep.24451.
2. Salem R, Lewandowski RJ, Kulik L, Wang E, Riaz A, Ryu RK, et al. Radioembolization results in longer time-to-progression and reduced toxicity compared with chemoembolization in patients with hepatocellular carcinoma. Gastroenterology. 2011;140:497–507.e2. doi:10.1053/j.gastro.2010.10.049.
3. Welsh JS, Kennedy AS, Thomadsen B. Selective Internal Radiation Therapy (SIRT) for liver metastases secondary to colorectal adenocarcinoma. Int J Radiat Oncol Biol Phys. 2006;66:S62–73. doi:10.1016/j.ijrobp.2005.09.011.
4. Campbell AM, Bailey IH, Burton MA. Analysis of the distribution of intra-arterial microspheres in human liver following hepatic yttrium-90 microsphere therapy. Phys Med Biol. 2000;45:1023–33.
5. Salem R, Thurston KG. Radioembolization with 90Yttrium microspheres: a state-of-the-art brachytherapy treatment for primary and secondary liver malignancies. Part 1: technical and methodologic considerations. J Vasc Interv Radiol. 2006;17:1251–78.
6. Lien WM, Ackerman NB. The blood supply of experimental liver metastases. II. A microcirculatory study of the normal and tumor vessels of the liver with the use of perfused silicone rubber. Surgery. 1970;68:334–40.
7. Vente MA, Nijsen JF, de Wit TC, Seppenwoolde JH, Krijger GC, Seevinck PR, et al. Clinical effects of transcatheter hepatic arterial embolization with holmium-166 poly(L-lactic acid) microspheres in healthy pigs. Eur J Nucl Med Mol Imaging. 2008;35:1259–71. doi:10.1007/s00259-008-0747-8.
8. Lin YC, Tsai SC, Hung GU, Lee JC, Huang YS, Lin WY. Direct injection of (188)Re-microspheres in the treatment of hepatocellular carcinoma: compared with traditional percutaneous ethanol injection: an animal study. Nuklearmedizin. 2005;44:76–80. doi:10.1267/NUKL05030076.
9. Liu L, Jiang Z, Teng GJ, Song JZ, Zhang DS, Guo QM, et al. Clinical and experimental study on regional administration of phosphorus 32 glass microspheres in treating hepatic carcinoma. World J Gastroenterol. 1999;5:492–505.
10. Amoui M, Pirayesh E, Akhlaghpoor S, Tolooee B, Poorbeigi H, Sheibani S. Correlation between CT/MRI and bremsstrahlung SPECT of 32P after radioembolization of hepatic tumors. Iran J Radiol. 2010;7:1–5.
11. Ahmadzadehfar H, Biersack HJ, Ezziddin S. Radioembolization of liver tumors with yttrium-90 microspheres. Semin Nucl Med. 2010;40:105–21. doi:10.1053/j.semnuclmed.2009.11.001.
12. Kennedy A, Nag S, Salem R, Murthy R, McEwan AJ, Nutting C, et al. Recommendations for radioembolization of hepatic malignancies using yttrium-90 microsphere brachytherapy: a consensus panel report from the radioembolization brachytherapy oncology consortium. Int J Radiat Oncol Biol Phys. 2007;68:13–23. doi:10.1016/j.ijrobp.2006.11.060.
13. Murthy R, Nunez R, Szklaruk J, Erwin W, Madoff DC, Gupta S, et al. Yttrium-90 microsphere therapy for hepatic malignancy: devices, indications, technical considerations, and potential complications. Radiographics. 2005;25 Suppl 1:S41–55. doi:10.1148/rg.25si055515.
14. Riaz A, Lewandowski RJ, Kulik LM, Mulcahy MF, Sato KT, Ryu RK, et al. Complications following radioembolization with yttrium-90 microspheres: a comprehensive literature review. J Vasc Interv Radiol. 2009;20:1121–30. doi:10.1016/j.jvir.2009.05.030. quiz 31.
15. Yip D, Allen R, Ashton C, Jain S. Radiation-induced ulceration of the stomach secondary to hepatic embolization with radioactive yttrium microspheres in the treatment of metastatic colon cancer. J Gastroenterol Hepatol. 2004;19:347–9.
16. Carretero C, Munoz-Navas M, Betes M, Angos R, Subtil JC, Fernandez-Urien I, et al. Gastroduodenal injury after radioembolization of hepatic tumors. Am J Gastroenterol. 2007;102:1216–20. doi:10.1111/j.1572-0241.2007.01172.x.
17. Leung TW, Lau WY, Ho SK, Ward SC, Chow JH, Chan MS, et al. Radiation pneumonitis after selective internal radiation treatment with intraarterial 90yttrium-microspheres for inoperable hepatic tumors. Int J Radiat Oncol Biol Phys. 1995;33:919–24.
18. Murthy R, Brown DB, Salem R, Meranze SG, Coldwell DM, Krishnan S, et al. Gastrointestinal complications associated with hepatic arterial yttrium-90 microsphere therapy. J Vasc Interv Radiol. 2007;18:553–62. doi:10.1016/j.jvir.2007.02.002.
19. Salem R, Parikh P, Atassi B, Lewandowski RJ, Ryu RK, Sato KT, et al. Incidence of radiation pneumonitis after hepatic intra-arterial radiotherapy with yttrium-90 microspheres assuming uniform lung distribution. Am J Clin Oncol. 2008;31:431–8. doi:10.1097/COC.0b013e318168ef65.
20. Atassi B, Bangash AK, Lewandowski RJ, Ibrahim S, Kulik L, Mulcahy MF, et al. Biliary sequelae following radioembolization with yttrium-90 microspheres. J Vasc Interv Radiol. 2008;19:691–7. doi:10.1016/j.jvir.2008.01.003.
21. Covey AM, Brody LA, Maluccio MA, Getrajdman GI, Brown KT. Variant hepatic arterial anatomy revisited: digital subtraction angiography performed in 600 patients. Radiology. 2002;224:542–7.
22. Ahmadzadehfar H, Sabet A, Biermann K, Muckle M, Brockmann H, Kuhl C, et al. The significance of 99mTc-MAA SPECT/CT liver perfusion imaging in treatment planning for 90Y-microsphere selective internal radiation treatment. J Nucl Med. 2010;51:1206–12. doi:10.2967/jnumed.109.074559.
23. Lenoir L, Edeline J, Rolland Y, Pracht M, Raoul JL, Ardisson V, et al. Usefulness and pitfalls of MAA SPECT/CT in identifying digestive extrahepatic uptake when planning liver radioembolization. Eur J Nucl Med Mol Imaging. 2012;39:872–80. doi:10.1007/s00259-011-2033-4.

24. Hamami ME, Poeppel TD, Muller S, Heusner T, Bockisch A, Hilgard P, et al. SPECT/CT with 99mTc-MAA in radioembolization with 90Y microspheres in patients with hepatocellular cancer. J Nucl Med. 2009;50:688–92. doi:10.2967/jnumed.108.058347.
25. Denecke T, Ruhl R, Hildebrandt B, Stelter L, Grieser C, Stiepani H, et al. Planning transarterial radioembolization of colorectal liver metastases with yttrium 90 microspheres: evaluation of a sequential diagnostic approach using radiologic and nuclear medicine imaging techniques. Eur Radiol. 2008;18:892–902. doi:10.1007/s00330-007-0836-2.
26. Dudeck O, Wilhelmsen S, Ulrich G, Lowenthal D, Pech M, Amthauer H, et al. Effectiveness of repeat angiographic assessment in patients designated for radioembolization using yttrium-90 microspheres with initial extrahepatic accumulation of technitium-99m macroaggregated albumin: a single center's experience. Cardiovasc Intervent Radiol. 2012;35:1083–93. doi:10.1007/s00270-011-0252-5.
27. Giammarile F, Bodei L, Chiesa C, Flux G, Forrer F, Kraeber-Bodere F, et al. EANM procedure guideline for the treatment of liver cancer and liver metastases with intra-arterial radioactive compounds. Eur J Nucl Med Mol Imaging. 2011;38:1393–406. doi:10.1007/s00259-011-1812-2.
28. Ahmadzadehfar H, Muckle M, Sabet A, Wilhelm K, Kuhl C, Biermann K, et al. The significance of bremsstrahlung SPECT/CT after yttrium-90 radioembolization treatment in the prediction of extrahepatic side effects. Eur J Nucl Med Mol Imaging. 2012;39:309–15. doi:10.1007/s00259-011-1940-8.
29. Ahmadzadehfar H, Sabet A, Muckle M, Wilhelm K, Reichmann K, Biersack HJ, et al. 99mTc-MAA/90Y-Bremsstrahlung SPECT/CT after simultaneous Tc-MAA/90Y-microsphere injection for immediate treatment monitoring and further therapy planning for radioembolization. Eur J Nucl Med Mol Imaging. 2011;38:1281–8. doi:10.1007/s00259-011-1751-y.
30. Mansberg R, Sorensen N, Mansberg V, Van der Wall H. Yttrium 90 Bremsstrahlung SPECT/CT scan demonstrating areas of tracer/tumour uptake. Eur J Nucl Med Mol Imaging. 2007;34:1887. doi:10.1007/s00259-007-0536-9.
31. Fabbri C, Sarti G, Cremonesi M, Ferrari M, Di Dia A, Agostini M, et al. Quantitative analysis of 90Y Bremsstrahlung SPECT-CT images for application to 3D patient-specific dosimetry. Cancer Biother Radiopharm. 2009;24:145–54. doi:10.1089/cbr.2008.0543.
32. Strahlenschutzkommission Sd. Radionuklidtherapie mittels selektiver intraarterieller Radiotherapie (SIRT) und intravasale Bestrahlung mit offenen Radionukliden. In: Strahlenschutzkommission, editor. Bonn; 2009
33. Sabet A, Ahmadzadehfar H, Muckle M, Haslerud T, Wilhelm K, Biersack HJ, et al. Significance of oral administration of sodium perchlorate in planning liver-directed radioembolization. J Nucl Med. 2011;52:1063–7. doi:10.2967/jnumed.110.083626.
34. Uliel L, Royal HD, Darcy MD, Zuckerman DA, Sharma A, Saad NE. From the angio suite to the gamma-camera: vascular mapping and 99mTc-MAA hepatic perfusion imaging before liver radioembolization – a comprehensive pictorial review. J Nucl Med. 2012;53:1736–47. doi:10.2967/jnumed.112.105361.
35. Van de Wiele C, Stellamans K, Brugman E, Mees G, De Spiegeleer B, D'Asseler Y, et al. Quantitative pretreatment VOI analysis of liver metastases. (99m)Tc-MAA SPECT/CT and FDG PET/CT in relation with treatment response to SIRT. Nuklearmedizin. 2013;52:21–7.
36. Kao YH, Tan EH, Teo TK, Ng CE, Goh SW. Imaging discordance between hepatic angiography versus Tc-99m-MAA SPECT/CT: a case series, technical discussion and clinical implications. Ann Nucl Med. 2011;25:669–76. doi:10.1007/s12149-011-0516-9.
37. Naymagon S, Warner RR, Patel K, Harpaz N, Machac J, Weintraub JL, et al. Gastroduodenal ulceration associated with radioembolization for the treatment of hepatic tumors: an institutional experience and review of the literature. Dig Dis Sci. 2010;55:2450–8. doi:10.1007/s10620-010-1156-y.
38. Lauenstein TC, Heusner TA, Hamami M, Ertle J, Schlaak JF, Gerken G, et al. Radioembolization of hepatic tumors: flow redistribution after the occlusion of intrahepatic arteries. Rofo. 2011;183:1058–64. doi:10.1055/s-0031-1281767.
39. McWilliams JP, Kee ST, Loh CT, Lee EW, Liu DM. Prophylactic embolization of the cystic artery before radioembolization: feasibility, safety, and outcomes. Cardiovasc Intervent Radiol. 2011;34:786–92. doi:10.1007/s00270-010-0021-x.
40. Chernyak I, Bester L, Freund J, Richardson M. Anterior abdominal wall uptake in intrahepatic arterial brachytherapy with yttrium-90 sir spheres for hepatic malignancy. Clin Nucl Med. 2008;33:677–80. doi:10.1097/RLU.0b013e318184b44f.
41. Kao YH, Tan AE, Khoo LS, Lo RH, Chow PK, Goh AS. Hepatic falciform ligament Tc-99 m-macroaggregated albumin activity on SPECT/CT prior to Yttrium-90 microsphere radioembolization: prophylactic measures to prevent non-target microsphere localization via patent hepatic falciform arteries. Ann Nucl Med. 2011;25:365–9. doi:10.1007/s12149-010-0464-9.
42. Ahmadzadehfar H, Mohlenbruch M, Sabet A, Meyer C, Muckle M, Haslerud T, et al. Is prophylactic embolization of the hepatic falciform artery needed before radioembolization in patients with 99mTc-MAA accumulation in the anterior abdominal wall? Eur J Nucl Med Mol Imaging. 2011;38:1477–84. doi:10.1007/s00259-011-1807-z.
43. Barentsz MW, Vente MA, Lam MG, Smits ML, Nijsen JF, Seinstra BA, et al. Technical solutions to ensure safe yttrium-90 radioembolization in patients with initial extrahepatic deposition of (99m)technetium-albumin macroaggregates. Cardiovasc Intervent Radiol. 2011;34:1074–9. doi:10.1007/s00270-010-0088-4.
44. Burgmans MC, Too CW, Kao YH, Goh AS, Chow PK, Tan BS, et al. Computed tomography hepatic arteriography has a hepatic falciform artery detection rate that is much higher than that of digital subtraction angiography and 99mTc-MAA SPECT/CT: implications for planning 90Y radioembolization? Eur J Radiol. 2012;81:3979–84. doi:10.1016/j.ejrad.2012.08.007.
45. Baba Y, Miyazono N, Ueno K, Kanetsuki I, Nishi H, Inoue H, et al. Hepatic falciform artery. Angiographic findings in 25 patients. Acta Radiol. 2000;41:329–33.
46. Leong QM, Lai HK, Lo RG, Teo TK, Goh A, Chow PK. Radiation dermatitis following radioembolization for hepatocellular carcinoma: a case for prophylactic embolization of a patent falciform artery. J Vasc Interv Radiol. 2009;20:833–36. doi:10.1016/j.jvir.2009.03.011.
47. Garin E, Lenoir L, Rolland Y, Edeline J, Mesbah H, Laffont S, et al. Dosimetry based on 99mTc-macroaggregated albumin SPECT/CT accurately predicts tumor response and survival in hepatocellular carcinoma patients treated with 90Y-loaded glass microspheres: preliminary results. J Nucl Med. 2012;53:255–63. doi:10.2967/jnumed.111.094235.
48. Flamen P, Vanderlinden B, Delatte P, Ghanem G, Ameye L, Van Den Eynde M, et al. Multimodality imaging can predict the metabolic response of unresectable colorectal liver metastases to radioembolization therapy with Yttrium-90 labeled resin microspheres. Phys Med Biol. 2008;53:6591–603. doi:10.1088/0031-9155/53/22/019.
49. Garin E, Lenoir L, Rolland Y, Laffont S, Pracht M, Mesbah H, et al. Effectiveness of quantitative MAA SPECT/CT for the definition of vascularized hepatic volume and dosimetric approach: phantom validation and clinical preliminary results in patients with complex hepatic vascularization treated with yttrium-90-labeled microspheres. Nucl Med Commun. 2011;32:1245–55. doi:10.1097/MNM.0b013e32834a716b.
50. Garin E, Lenoir L, Edeline J, Laffont S, Mesbah H, Poree P, et al. Boosted selective internal radiation therapy with 90Y-loaded glass microspheres (B-SIRT) for hepatocellular carcinoma patients: a new personalized promising concept. Eur J Nucl Med Mol Imaging. 2013;40:1057–68. doi:10.1007/s00259-013-2395-x.
51. Salem R, Lewandowski RJ, Gates VL, Nutting CW, Murthy R, Rose SC, et al. Research reporting standards for radioembolization of

hepatic malignancies. J Vasc Interv Radiol. 2011;22:265–78. doi:10.1016/j.jvir.2010.10.029.
52. Lau WY, Leung TW, Ho S, Chan M, Leung NW, Lin J, et al. Diagnostic pharmaco-scintigraphy with hepatic intra-arterial technetium-99m macroaggregated albumin in the determination of tumour to non-tumour uptake ratio in hepatocellular carcinoma. Br J Radiol. 1994;67:136–9.
53. Fox RA, Klemp PF, Egan G, Mina LL, Burton MA, Gray BN. Dose distribution following selective internal radiation therapy. Int J Radiat Oncol Biol Phys. 1991;21:463–7.
54. Burton MA, Gray BN, Klemp PF, Kelleher DK, Hardy N. Selective internal radiation therapy: distribution of radiation in the liver. Eur J Cancer Clin Oncol. 1989;25:1487–91.
55. Ho S, Lau WY, Leung TW, Chan M, Ngar YK, Johnson PJ, et al. Partition model for estimating radiation doses from yttrium-90 microspheres in treating hepatic tumours. Eur J Nucl Med. 1996;23:947–52.
56. Chiesa C, Maccauro M, Romito R, Spreafico C, Pellizzari S, Negri A, et al. Need, feasibility and convenience of dosimetric treatment planning in liver selective internal radiation therapy with (90)Y microspheres: the experience of the National Tumor Institute of Milan. Q J Nucl Med Mol Imaging. 2011;55:168–97.
57. Chiesa C, Mira M, Maccauro M, Romito R, Spreafico C, Sposito C, et al. A dosimetric treatment planning strategy in radioembolization of hepatocarcinoma with 90Y glass microspheres. Q J Nucl Med Mol Imaging. 2012;56:503–8.
58. Jiang M, Fischman A, Nowakowski F, Heiba S, Zhang Z, Knesaurek K, et al. Segmental perfusion differences on paired Tc-99 m Macroaggregated Albumin (MAA) hepatic perfusion imaging and Yttrium-90 (Y-90) bremsstrahlung imaging studies in SIR-Sphere radioembolization: associations with Angiography. J Nucl Med Radiat Ther. 2012;3:122.
59. Wondergem M, Smits ML, Elschot M, de Jong HW, Verkooijen HM, van den Bosch MA, et al. 99mTc-macroaggregated albumin poorly predicts the intrahepatic distribution of 90Y resin microspheres in hepatic radioembolization. J Nucl Med. 2013;54:1294–301. doi:10.2967/jnumed.112.117614.
60. Basciano C, Kleinstreuer C, Kennedy A. Computational fluid dynamics modeling of 90Y microspheres in human hepatic tumors. J Nucl Med Radiat Ther. 2011;2:1–6.
61. Walrand S, Lhommel R, Goffette P, Van den Eynde M, Pauwels S, Jamar F. Hemoglobin level significantly impacts the tumor cell survival fraction in humans after internal radiotherapy. EJNMMI Res. 2012;2:20. doi:10.1186/2191-219X-2-20.
62. Gupta T, Virmani S, Neidt TM, Szolc-Kowalska B, Sato KT, Ryu RK, et al. MR tracking of iron-labeled glass radioembolization microspheres during transcatheter delivery to rabbit VX2 liver tumors: feasibility study. Radiology. 2008;249:845–54. doi:10.1148/radiol.2491072027.
63. Walrand S, Hesse M, Demonceau G, Pauwels S, Jamar F. Yttrium-90-labeled microsphere tracking during liver selective internal radiotherapy by bremsstrahlung pinhole SPECT: feasibility study and evaluation in an abdominal phantom. EJNMMI Res. 2011;1:32. doi:10.1186/2191-219X-1-32.
64. D'Asseler Y. Advances in SPECT imaging with respect to radionuclide therapy. Q J Nucl Med Mol Imaging. 2009;53:343–7.
65. Minarik D, Sjogreen Gleisner K, Ljungberg M. Evaluation of quantitative (90)Y SPECT based on experimental phantom studies. Phys Med Biol. 2008;53:5689–703. doi:10.1088/0031-9155/53/20/008.
66. Lassmann M. Dosimetry of short-ranged radionuclides. Nuklearmedizin. 2010;49 Suppl 1:S46–9.
67. Rong X, Du Y, Frey EC. A method for energy window optimization for quantitative tasks that includes the effects of model-mismatch on bias: application to Y-90 bremsstrahlung SPECT imaging. Phys Med Biol. 2012;57:3711–25. doi:10.1088/0031-9155/57/12/3711.
68. Ito S, Kurosawa H, Kasahara H, Teraoka S, Ariga E, Deji S, et al. (90)Y bremsstrahlung emission computed tomography using gamma cameras. Ann Nucl Med. 2009;23:257–67. doi:10.1007/s12149-009-0233-9.
69. Knesaurek K, Machac J, Muzinic M, DaCosta M, Zhang Z, Heiba S. Quantitative comparison of yttrium-90 (90Y)-microspheres and technetium-99 m (99mTc)-macroaggregated albumin SPECT images for planning 90Y therapy of liver cancer. Technol Cancer Res Treat. 2010;9:253–62.
70. Sebastian AJ, Szyszko T, Al-Nahhas A, Nijran K, Tait NP. Evaluation of hepatic angiography procedures and bremsstrahlung imaging in selective internal radiation therapy: a two-year single-center experience. Cardiovasc Intervent Radiol. 2008;31:643–9. doi:10.1007/s00270-008-9298-4.
71. Minarik D, Ljungberg M, Segars P, Gleisner KS. Evaluation of quantitative planar 90Y bremsstrahlung whole-body imaging. Phys Med Biol. 2009;54:5873–83. doi:10.1088/0031-9155/54/19/014.
72. Elschot M, Vermolen BJ, Lam MG, de Keizer B, van den Bosch MA, de Jong HW. Quantitative comparison of PET and Bremsstrahlung SPECT for imaging the in vivo yttrium-90 microsphere distribution after liver radioembolization. PLoS One. 2013;8:e55742. doi:10.1371/journal.pone.0055742.
73. Lau WY, Ho S, Leung TW, Chan M, Ho R, Johnson PJ, et al. Selective internal radiation therapy for nonresectable hepatocellular carcinoma with intraarterial infusion of 90yttrium microspheres. Int J Radiat Oncol Biol Phys. 1998;40:583–92.
74. Grosser OS, Nultsch M, Laatz K, Ulrich G, Seidensticker R, Pethe A, et al. Radioembolization with (90)Y-labeled microspheres: post-therapeutic therapy validation with Bremsstrahlung-SPECT. Z Med Phys. 2011;21:274–80. doi:10.1016/j.zemedi.2011.05.002.
75. Minarik D, Sjogreen-Gleisner K, Linden O, Wingardh K, Tennvall J, Strand SE, et al. 90Y Bremsstrahlung imaging for absorbed-dose assessment in high-dose radioimmunotherapy. J Nucl Med. 2010;51:1974–8. doi:10.2967/jnumed.110.079897.
76. Rong X, Du Y, Ljungberg M, Rault E, Vandenberghe S, Frey EC. Development and evaluation of an improved quantitative (90)Y bremsstrahlung SPECT method. Med Phys. 2012;39:2346–58. doi:10.1118/1.3700174.
77. van Elmbt L, Vandenberghe S, Walrand S, Pauwels S, Jamar F. Comparison of yttrium-90 quantitative imaging by TOF and non-TOF PET in a phantom of liver selective internal radiotherapy. Phys Med Biol. 2011;56:6759–77. doi:10.1088/0031-9155/56/21/001.
78. Lhommel R, van Elmbt L, Goffette P, Van den Eynde M, Jamar F, Pauwels S, et al. Feasibility of 90Y TOF PET-based dosimetry in liver metastasis therapy using SIR-Spheres. Eur J Nucl Med Mol Imaging. 2010;37:1654–62. doi:10.1007/s00259-010-1470-9.
79. Willowson K, Forwood N, Jakoby BW, Smith AM, Bailey DL. Quantitative (90)Y image reconstruction in PET. Med Phys. 2012;39:7153–9. doi:10.1118/1.4762403.
80. Kao YH, Tan EH, Ng CE, Goh SW. Yttrium-90 time-of-flight PET/CT is superior to Bremsstrahlung SPECT/CT for postradioembolization imaging of microsphere biodistribution. Clin Nucl Med. 2011;36:e186–7. doi:10.1097/RLU.0b013e31821c9a11.